PROCEEDINGS OF SPIE

SPIEDigitalLibrary.org/conference-proceedings-of-spie

One-dimensional local binary pattern based color descriptor to classify stress values from photoelasticity videos

Juan C. Briñez de León, Domingo Mery, Alejandro Restrepo M., John W. Branch

Juan C. Briñez de León, Domingo Mery, Alejandro Restrepo M., John W. Branch, "One-dimensional local binary pattern based color descriptor to classify stress values from photoelasticity videos," Proc. SPIE 11136, Optics and Photonics for Information Processing XIII, 1113607 (6 September 2019); doi: 10.1117/12.2528418

SPIE.

Event: SPIE Optical Engineering + Applications, 2019, San Diego, California, United States

One-dimensional local binary pattern based color descriptor to classify stress values from photoelasticity videos

Juan C. Briñez de León*[a,c,d], Domingo Mery[b], Alejandro Restrepo M.[c], John W. Branch[a]

[a] Departamento de Ingeniería Electrónica, Facultad de Ingenierías, Institución Universitaria Pascual Bravo, Medellín, Antioquia, Colombia.
[b] Department of Computer Science, Pontificia Universidad Católica de Chile, Santiago de Chile, Chile.
[c] Grupo de Promoción e Investigación en Mecánica Aplicada GPIMA, Universidad Nacional de Colombia, Medellín, Colombia.
[d] Grupo de Investigación en Inteligencia Artificial, GIDIA, Universidad Nacional de Colombia, Medellín, Colombia.

ABSTRACT

Evaluating the stress distribution in structures under temporal loads is being carry out by many of the engineering applications such as: impacts, cracks, bending, thermal-transient and other. In those cases, conventional photoelasticity techniques are more complex to evaluate the stress field because of their complicated and expensive experiments, quantity of computational procedures, and their time by time analysis. However, dynamic photoelasticity experiments produce temporal information, such as color variations, which could be analyzed, described, and classified in order to perform a whole stress field evaluation. In this paper, the one-dimensional local binary patterns (1D-LBP) are used to describe such color variations and use them to identify the stress values they belong. For different experimental configurations, this proposal achieved an accuracy of 98% when evaluating the stress field of cases with similar light sources than with a reference experiment, and 92% for experiments with other light conditions. These results make this descriptor able to determine categorical stress maps from a photoelasticity video itself, which significantly opens new opportunities to simplify the experimental and computational operations that limit the stress evaluation process in line with the dynamic experiment.

Keywords: Digital photoelasticity, temporal color analysis, 1D-LBP, artificial neural networks.

1. INTRODUCTION

Digital photoelasticity is an experimental technique used for evaluating the stress distribution in structures subjected to mechanical loads [1]. This technique has been highlighted between the experimental stress evaluation methods because its visual capability to represent the stress information through digital images with spatial color fringe patterns. In those cases, the stress field is recovered by developing computational processes over such patterns. However, there are some drawbacks that affect the photoelasticity application in dynamic contexts. These limitations are usually related to complicated experiments, processing techniques, multiple acquisitions, correction strategies, complex geometries, and unwrapping algorithms [2].

Most of difficulties for carrying out photoelasticity techniques in dynamic experiments come from the fact that fringe patterns not only vary spatially, but also in time with every load increment [3]. This makes the photoelasticity techniques, additional to conventional limitations in static conditions, be dependent on the acquisition and processing time. For dealing with these constrains, photoelasticity studies have oriented their efforts to evaluate the stress field by acquiring and processing one single image per load value, as it is the case of Twelve fringe photoelasticity TFP [4], regularized phase tracking RPT [5], and multiple polarized acquisition [6]. Then, the procedure is repeated, frame by frame, per every load variation.

Color comparison based techniques highlight in digital photoelasticity to evaluate the stress field [7]. However, they must be tuned per every experimental configuration because of the sensibility that color intensities experience with each

Optics and Photonics for Information Processing XIII, edited by Khan M. Iftekharuddin, Abdul A.S. Awwal, Victor H. Diaz-Ramirez, Andrés Márquez, Proc. of SPIE Vol. 11136
1113607 · © 2019 SPIE · CCC code: 0277-786X/19/$21 · doi: 10.1117/12.2528418

element interacting with the experiment [8, 9]. In this research line, automatic methods based on inverse problems have been proposed [10]. Notwithstanding, the need of re-train the neural networks, when changes in the experimental conditions, makes the technique complex to apply in time-dependent contexts.

On the other hand, new tendencies in dynamic photoelasticity studies have reported that temporal color variations contain information that could be related to the stress field, as it is the case of the automatic identification of the stress concentration zones into the loaded structure [11, 12]. In those cases, besides being color based strategies, the stress field quantification is not performed. There, the temporal color information, at each specific position into the structure, can be assumed as 1D-temporal signal that vary dynamically with respect to other structure positions. These finds have opened new research possibilities in order to analyze such signals for avoiding the color experimental dependence and quantify the stress field in automatic way.

In relation to signal dynamic analysis, literature report different research works that could be explored in digital photoelasticity studies for describing the temporal color variations, and associate them to stress values, such as: time-domain, frequency-domain, time–frequency domain and nonlinear methods [13]. Nevertheless, much of such descriptors produce feature that require complex classifiers to discriminate between different dynamics. Thus, they will not be objective of this work. In this case, the main goal is to evaluate the possibility of representing the dynamic of the temporal color variations enough good to differentiate between stress values accurately.

As a response to the need described previously, one-dimensional local binary pattern (1D-LBP) is a signal descriptor that has proven to be quite effective for various type of applications [14–16]. This descriptor was initially proposed for carry out texture analysis in images [17], but its performance in signal analysis is catching the attention of the researchers in different engineering areas. Notwithstanding, literature report few works in optical areas that evaluate effectiveness of 1D-LBP signal descriptor to differentiate between a variety of temporal behavior, as it is the case of temporal color variations in dynamic photoelasticity.

In this paper, we propose to evaluate the stress field in dynamic photoelasticity experiments by implementing the 1D-LBP signal descriptor, and apply it to the color variation signals resulting of every structure position into the dynamic experiment. This procedure is carry out in various steps. The first one correspond to the data generations by simulating the optic phenomenon which occur in dynamic photoelasticity. There, different light sources and a couple of structures are considered. The second step accounts for implementing the 1D-LBP to perform the temporal color description of data generated in the previous step. As third step, a classifier is trained to differentiate between dynamics in temporal color variations, and associate them to different stress categories. In this case, an artificial neural network (ANN) is trained by using signals of one single experimental conditions, and then evaluated by considering signals of all the experimental considerations. Finally, results, analysis and conclusions are presented.

2. METHODS AND PROCEDURES

2.1 Photoelasticity images

Photoelasticity images reveal the internal forces interacting into a loaded structure. This information corresponds to the stress distributed into the body geometry, and its evaluation allows users identify the mechanical response that a specific material experience to the experimental conditions [18]. This phenomenon is possible due to there exist materials that experience double refraction indexes (Birefringent) when they are under stress. In those cases, the principal stress difference and principal stress direction in every position of the structure modify the optical response to the light transmission, as indicated in (1).

$$\delta(x,y) = \frac{2\pi h C[\sigma_1(x,y) - \sigma_2(x,y)]}{\lambda} \tag{1}$$

In that case, ' $\sigma_1(x,y)$ ' and ' $\sigma_2(x,y)$ ' represent the principal stress components for each ' (x,y) ' position into the structure. The unknowns ' h ', ' C ' and ' λ ' represent the thickness, stress optic coefficient, and light wavelength, respectively. Likewise, ' $\delta(x,y)$ ' represents the phase delay of the light when traveling through the body [1]. The optic relationship between the principal stress difference and the phase delay is called as "Stress optic law", and it is observed by lighting the loaded structure thorough a polariscope arrangement, as shown in the Figure 9 for a configuration of circular polariscope. In those arrangements, the emergent colors are functions of the light source spectral contents, optic

elements in the polariscope, spatial stress distribution (principal stress difference and direction), and the relative spectral response in the camera sensor [5].

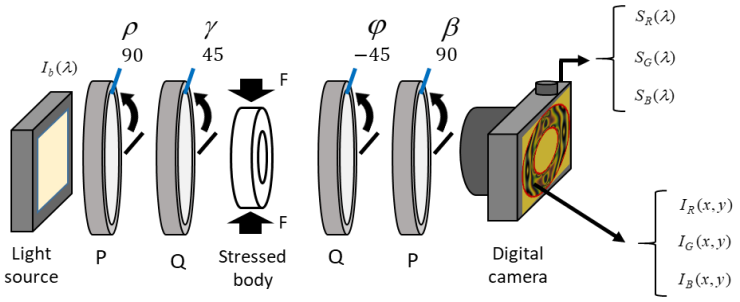

Figure 1. Scheme of a circular polariscope.

Where, $I_b(\lambda)$ is the relative spectral content of the light source. In this case, 'ρ', 'γ', 'φ' and 'β' represent the rotation angles of the first linear polarizer 'P', first quarter wave plate 'Q', second quarter wave plate 'Q', and second linear polarizer 'P', respectively. Likewise, '$\delta(x,y)$' and '$\theta(x,y)$' are the principal stress difference and direction, respectively [2]. Hence, '$S_R(\lambda)$', '$S_G(\lambda)$' and '$S_B(\lambda)$' account for the relative spectral response of the camera sensor in the 'R', 'G' and 'B' color components, respectively. The emergent intensities are '$I_R(x,y)$', '$I_G(x,y)$' and '$I_B(x,y)$' for red, green and blue color channels, respectively.

For an easy intensity representation, photoelasticity techniques that use one single image setup the polariscope elements to bright or dark field configuration. In the bright field case, the polariscope elements are rotated as follow: '$\rho = 90$', '$\gamma = 45$', '$\varphi = -45$' and '$\beta = 90$'. Then, the emergent intensities in the red channel can be represented as (2). This equation considers a term '$I_a(\lambda)$' for representing the background light during the experiment. Emergent intensities for remaining color components can be obtained similarly by using the relative spectral response of the camera in the green and blue color channels. To this, it is assumed wavelengths between '$\lambda_1 = 390\text{nm}$' and '$\lambda_2 = 760\text{nm}$'. Similarly, the rectangular coordinates 'x' and 'y' are moved spatially between rows and columns, respectively.

$$I_R(x,y) = \frac{1}{\lambda_2 - \lambda_1} \int_{\lambda_1}^{\lambda_2} [I_a(\lambda) + \frac{I_b(\lambda)}{2} * [1 + \cos\delta(x,y,\lambda)]] * S_R(\lambda) d\lambda \tag{2}$$

Although digital photoelasticity images are often acquired experimentally, the complex configuration, cost of optics elements, environmental conditions, and technological advances have made researchers in photoelasticity explore their new proposals by simulating the experiments through computational procedures. In such cases, analytical models of structures under loads are developed to generate the stress field. Hence, disk and ring under diametric compression are the models more used in digital photoelasticity [19, 20]. The Figure 2 represents the process for generating the synthetic images. To make the process more real, these images consider the Bayer and demosaicking effect proposed in [21].

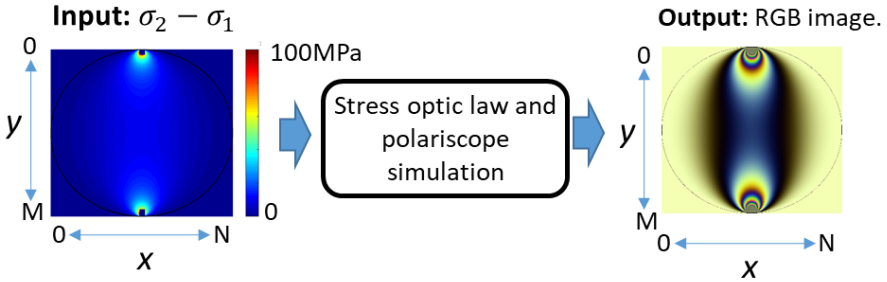

Figure 2. Scheme of a circular polariscope.

2.2 Temporal color variations in dynamic photoelasticity

Dynamic photoelasticity generally is seen as experimental cases some where the load applied to the structure '$P(t)$' is time-dependent [3]. In most of those cases, the temporal load behavior is considered in augmentation, and its optic effect is recorded through videos or sequences of digital images, as it is illustrated by the Figure 3 for a disk under temporal diametric compression. Hence, every pixel position into the sequence produce a temporal signal containing the information about the three color components, and similar size than load steps.

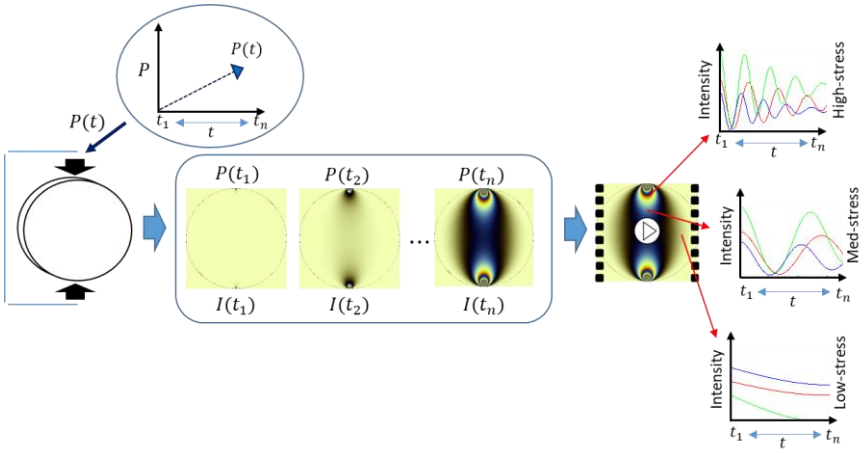

Figure 3. Scheme of sequence of images in dynamic photoelasticity.

As was presented above, in sequence of photoelasticity images, the temporal color behavior varies with respect to the stress zones into the loaded structure. The color modulation shows dynamic with more oscillations in high stress concentration zones, and the opposite for low stress concentration zones. Although such behavior is a tendency in dynamic photoelasticity experiments, the polariscope configuration, light sources, camera sensors, and load curve modify the color information into the sequence of images, as presented by the Figure 4 for a static into two image sequences generated considering different light sources. In the remaining part of the manuscript, the temporal color signal, in each one of the color components, will be expressed in discrete representation as $R[n]$, $G[n]$, and $B[n]$ for red, green, and blue, respectively. Where, n is the discrete representation of every load step.

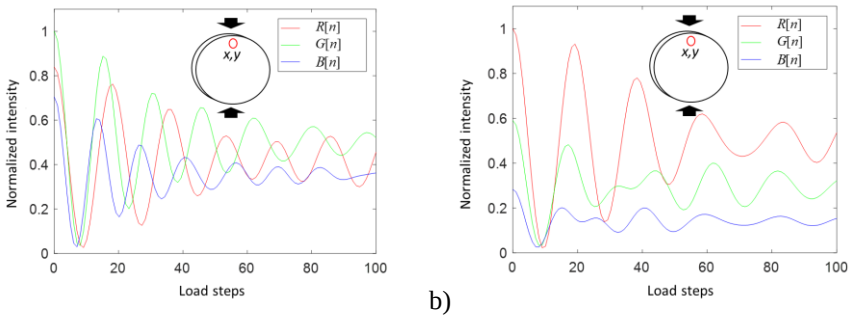

Figure 4. Temporal color signals in position (x, y) into the disk under diametric compression, but visualized using two different light sources. a) Experiment using white led, and b) Experiment using incandescent.

As a conventional representation of the temporal color dynamics, our approach generates feature vectors per every pixel position into the sequence of images. This process is developed by concatenating the raw color temporal variations obtained per each color component such pixel positions. With this exercise, the dynamic of the temporal color variation is represented by a feature vector of 1080 elements. In this case, 360 elements per each RGB color channel. In this work, the raw temporal color representation will be used as a reference point to evaluate the stress from dynamic color representations.

2.3 One-dimensional local binary pattern to describe the color variation (1D-LBP)

Initially, the bi-dimensional Local Binary Patterns (2D-LBP) were proposed for describing the texture information in gray images [17]. Such proposal gained importance between the scientist community by its potential of being gray scale and rotation invariant, allowing users improve the accuracy to recognize patterns from images. The success of the 2D-LBP has made the approach be extended to problems of different dimensions, such as the case of one-dimensional signals represented by 1D–LBP. This descriptor has the capability of representing the nature dynamic of one-dimensional signals, and use it to discriminate between specifics patterns [14]. In this paper, we use the 1D-LBP to describe the temporal color variations for every pixel position into the sequence of photoelasticity images. The main goal of this technique lies in the ability to represent the color information, in every sampled step, into new values coming from the relationship between every signal element and some past and future signal observations. This process is carried out, time by time, for all the intensity elements contained into the RGB signals.

The 1D-LBP feature vector generation, which represent the dynamic behavior of the color variations, start from extracting a new data vector ' R_2 ' with 8 elements around every temporal sample into the color variation R[n]. In such cases, the new vector contains four previous and four posterior elements, as represented by (3). There, the unknown 'k' represents the sample number into the temporal signal that is going to be converter. The second step accounts for obtaining information of the relationship between every element of the previous vector, and the evaluated sample. This process is performed through the subtraction of the previous generated vector, and the element into the interest position, as represented by (4). Next, a new data vector R_4 is generated according to the positive and negative subtraction results, as it is indicated by (5). Finally, a scalar value is obtained by transforming the previous binary vector into decimal, as indicated by (6). In these equation, the explanation only considers the red color channel R, as it is illustrated by the Figure 5. Nevertheless, Color channels G an B could be represented in similar way.

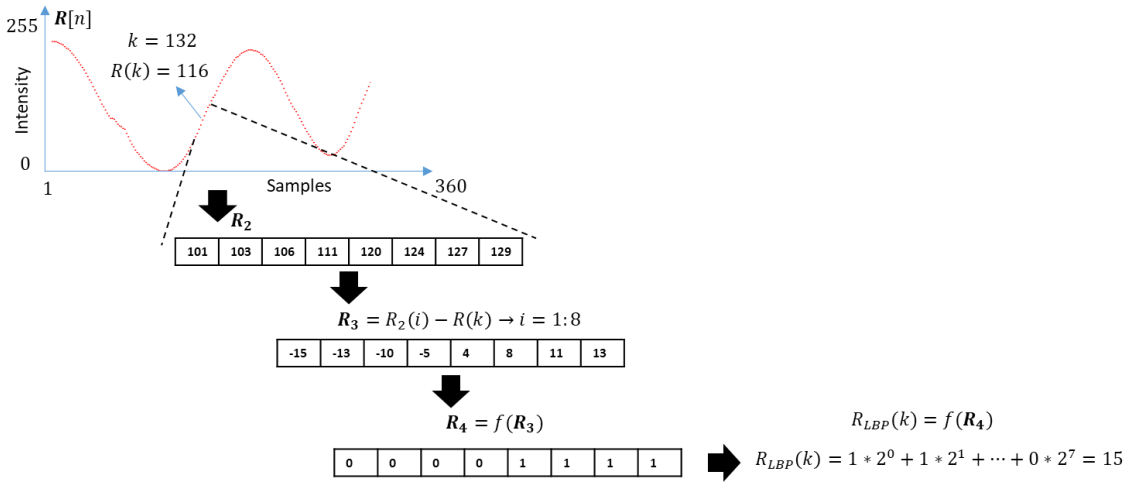

Figure 5. Representation of the LBP values calculation for a temporal sample into the red color channel.

$$R_2 = R[k+4, k+3, k+2, k+1, k-1, k-2, k-3, k-4] \tag{3}$$

$$R_3 = R_2 - R(k) \tag{4}$$

$$R_4(i) = \begin{cases} 1, if \rightarrow R_3(i) \geq 0 \\ 0, otherwise \end{cases}, \text{ for } i \text{ from 1 to 8.} \tag{5}$$

$$R_{LBP}(k) = \sum_{i=1}^{i=8} R_4(i) * 2^{i-1} \tag{6}$$

Although the new 1D-LBP signal contain the information about the local activity in every position and its previous and posterior times, classification applications have shown better performance when representing the original signal through

histograms generated from its 1D-LBP distributions [15]. In this paper, we calculate, channel by channel, the 1D-LBP signals initially, and then, we obtain their histograms, as it is indicated in the Figure 6 for R channel. Finally, the histograms from each color component are concatenated into one single data vector. In this exercise, the four initial and four final elements are not considered for the final 1D-LBP feature vector because, the generation process overlaps the original dimension of the interest signal.

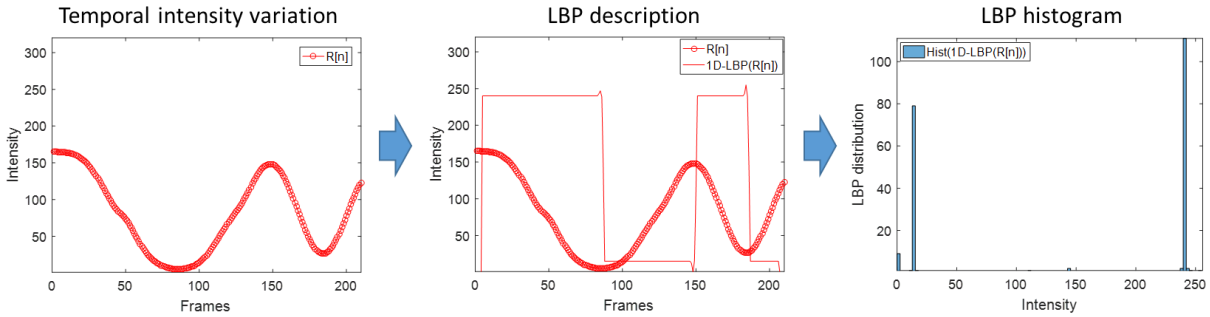

Figure 6. Scheme for representing the temporal color variation through 1D-LBP histograms.

2.4 Approach

Methodology proposed in this paper is presented by the block diagram in the Figure 7. Our approach involves an initial stage for the dataset generation using the simulation of the stress-optic relationship. The second block decomposes the image sequences into RGB temporal signals. This stage is followed by the 1D-LBP description, and its histogram generations. In the four stage, the training process of a classifier based on artificial neural networks is developed. After that, testing and validation stages are implemented.

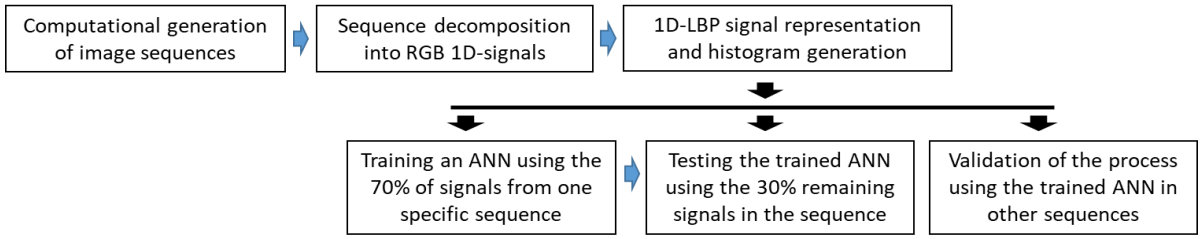

Figure 7. Block diagram of the proposed approach showing information fusion at the feature level.

This first block into the approach is proposed considering two analytical stress models, disk and ring under diametric compression. In those models, the load increments were applied as a linear curve sampled in 360 steps from 0 to 4500N in the disk, and 3800N in the ring case. Disk and ring diameter was 50mm. The ring inner diameter was 25mm. Both thicknesses were 10mm. For imaging the stress optic phenomenon, a bright field polariscope configuration was implemented. Hence, the relative spectral content of three light sources were used separately: fluorescent 'L1', incandescent 'L2', and Philip led 'L3'. As camera sensor, the relative spectral response of the Thorlab 'DCC3260C' sensor was used. At total, six photoelasticity sequences with '360' images each one were generated. This indicates that each color signal is composed by 360 elements. The image resolution was 512x512 pixels.

For the sequence decompositions, a pixel by pixel displacement was done to extract a 1D-signal per every position into the structure. In those cases, the background intensities were not taken into account. In this paper, the RGB information produced signals per every color channel. With this information, the histograms of 1D-LBP were obtained as explained in the previous section. Then, a concatenated vector is generated with the histograms of the three color channels. There, every histogram contributed with 255 data placed according to the red, green, and blue color channels, respectively. This process produced a feature vector of 765 data length.

Posterior to the signal representations, their association to different stress categories was proposed. To this stage, a categorical stress map (Ground-truth) was generated by discretizing the analytic stress field into for stress categories such as: critical, high, medium and low. Those categories were generated by taking into account different fringe orders

into the stress values, as it is represented in the Figure 8. The idea of such exercise was to provide a reference stress class for every RGB color signal.

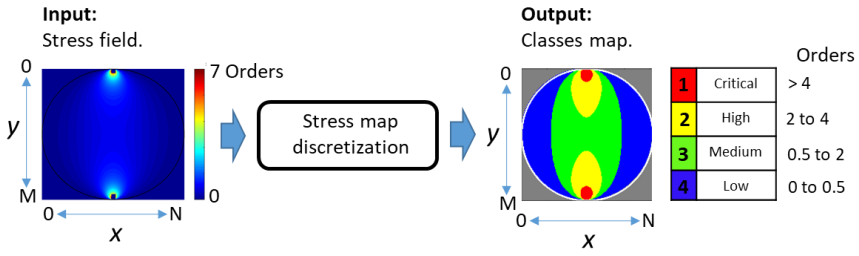

Figure 8. Representation of the stress class generation.

With the objective to detect the stress values from temporal color variations, a multilayer perceptron ANN with ten hidden layers was trained in five hundred epochs by using the descendent gradient, a sigmoid activation function, and the 1D-LBP histograms as input of 765 data length, as it is represented in the Figure 9. In this case, the image sequence for the disk lighting with fluorescent light source and recorded with the Thorlab cam was subsampled to 50% of the spatial positions, as it is indicated by the Figure 10. Then, the training process was only applied over the 70% of such division. In the testing case, the performance of the trained ANN was evaluated by detecting the stress categories for the remaining 30% of the signals contained in the subsampled dataset.

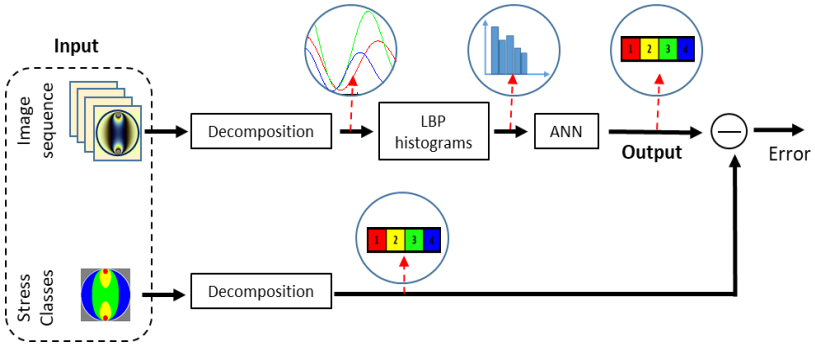

Figure 9. Scheme of the training process for detecting the stress classes by using a neural network.

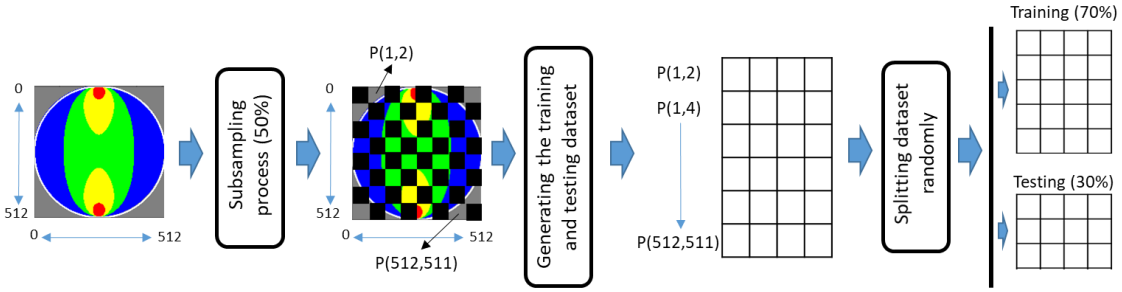

Figure 10. Scheme of the data set organization for training and testing the ANN.

Finally, the validation stage we propose in this paper is based on the prediction of all the stress categories (Stress field) related to the whole positions into the sequence of photoelasticity images. This exercise is carried out for evaluating the prediction performance in dynamic cases with experimental conditions quite different to such used as the reference to train the ANN. This indicates that the network trained with a half of the data from the sequence generated with the fluorescent light source in the disk model will be used to predict the complete stress map of this sequence, sequences generated for the ring analytic stress model, and sequences for both models considering two additional light sources. The obtained results by using the 1D-LBP descriptor will be compared with the stress detection carried out by using conventional representation of the of the RGB signals.

3. RESULTS AND ANALYSIS

In this section, obtained results are presented in terms of the performance about the complete stress map predicted from the temporal RGB color variations in all the pixel position of the sequences. However, it has to be mentioned that the training and testing process using the subsampled dataset performed an accuracy around the 99%. When using the trained ANN to predict the complete stress map from the image sequence of the dick under lighting with the fluorescents light source, the accuracy was 98.02%. This result can be evidenced by comparing the predicted stress map with respect to the reference stress map, and analyzing the precision values to identify the classes with better performance, as it is presented in the Figure 11.

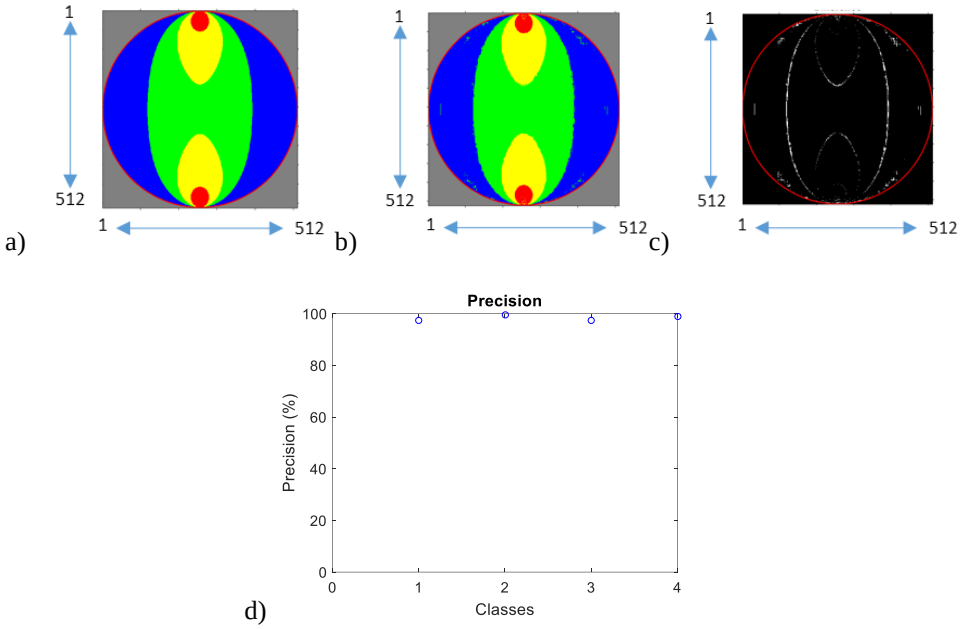

Figure 11. Predicted stress map by using the 1D-LBP color descriptor and a pre-trained network. a) Reference map, b) Predicted stress classes, c) Difference between predicted and reference stress map, and d) Precision per stress classes.

By analyzing the previous results, the difference between the reference and the predicted class map showed that bigger errors occur in the class transition regions. However, the precision values indicate that detecting all classes, for this kind of experiment, report high accuracy. Instead, the accuracy for sequences of the same stress model, and lighted with different light sources tends to reduce the accuracy. Notwithstanding, it continues being over the 93%. In these cases, the precision reports indicate that most of the errors are generated the class for the critical and high stress value, as it is presented in the Figure 12. This behavior could be attributed to the fact that such zones produce color dynamics with over modulation.

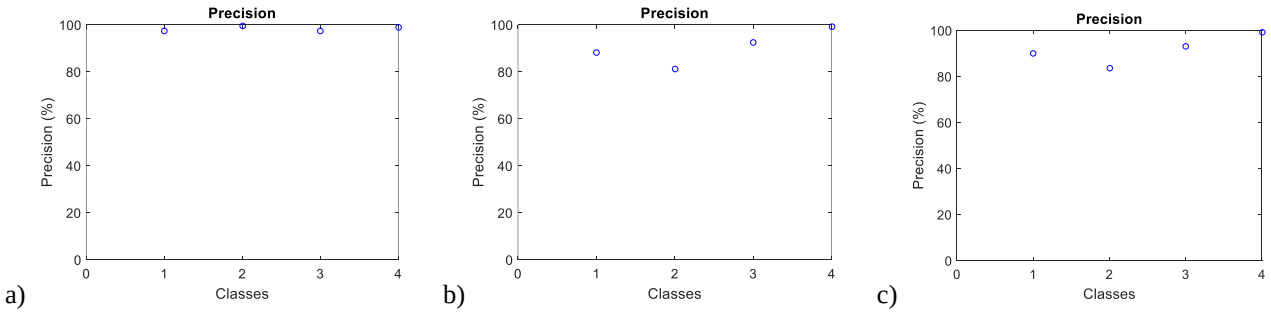

Figure 12. Precision report for stress map predictions of the disk under diametric compression when lighting with a) Fluorescent light source, b) Incandescent light source, and c) White led.

Sequences of images from the ring under diametric compression where evaluated with similar accuracy than the disk under compression. These results are presented in the Table 1. There, it can be observed that the trained ANN is able to predict the stress maps of different experimental conditions maintaining the accuracy over 92% in the worst of the experimental cases. Which in this case is the prediction of the stress map from sequences generated by using the incandescent light source. This result could be attributed to the color attenuation effect introduced by the spectral interaction between the light source and camera sensor.

Table 1. Accuracy report for prediction of the stress maps from different analytic models, spectral conditions, and description strategy.

	Accuracy predicting the stress maps in different experimental conditions					
	Disk under compression			Ring under compression		
Strategy	Fluorescent	Incandescent	White led	Fluorescent	Incandescent	White led
LBP + ANN	99.42%	93.68%	94.71%	98.44%	92.92%	93.74%
Raw color + ANN	92.79%	69.36	78.12%	89.68%	43.42	66.54%

As was additionally presented in above table, results of predicting the stress maps by using the raw color as dynamic descriptor, and the same classification strategy, developed low accuracy in comparison with the obtained with our proposal. In that case, sequences from the fluorescent light source report the highest accuracy. It is almost 7% less than the 1D-LBP strategy. But, the accuracy for other light sources is relatively low. This result could be attributed to the fact that dynamic description based on raw color makes the ANN develop high accuracy only for similar datasets than used to train the ANN, as it is the case of fluorescent light source. But, the such ANN perform bad when predicting the stress form data different light conditions. Over all, because that variation makes the color dynamic behave different into the RGB color space.

As a summary of the results, it could be said that although the raw color histograms are able to detect the stress values with high accuracy when evaluating the same experimental condition used to train the network, the accuracy gets reduced considerably when evaluating different experimental parameters, such as light sources. Notwithstanding, when comparing such result with the 1D-LBP strategy, it can be seen that the accuracy is maintained over the 92% in the worst of the cases. This means that this kind of descriptor allow users to reduce the problem of the experimental variations during the image acquisition process. In all the cases it is noteworthy that detection problems, in such manner, could be associated to the limits between the stress classes. These problems are more evident for the critical and high stress categories, and they could tend to occur for light sources that cause over-modulation of colors.

4. CONCLUSIONS

Stress field of structures subjected to time-dependent loads was evaluated in this paper by describing the dynamic of the temporal color variations in every pixel position into a sequence of photoelasticity images. Here, the color description was based on features derived from 1D-local binary patterns. For different experimental configurations, such as spectral content of the light sources, the proposed descriptor was capable of representing the temporal color variations, which are useful for differentiate between stress values. This behavior is consistent in comparison with techniques as raw color histograms, which only produce high accuracy when evaluating the same experimental conditions used for tuning the classifier parameters. However, it is necessary to consider the evaluation of this proposal on a bigger dataset that contain more experimental variations.

One of the most relevant contribution of the 1D-local binary patterns based color descriptor lies in the fact that a single experimental condition could be enough to train a classifier, and then, use it to evaluate the stress field in different experimental scenarios. These results make this descriptor able to determine categorical stress maps from a photoelasticity video itself, which significantly opens new opportunities to simplify the experimental and computational operations that limit the stress evaluation process in line with the dynamic experiment.

REFERENCES

[1] Ramesh, K., Kasimayan, T., & Neethi Simon, B. Digital photoelasticity–A comprehensive review. The Journal of Strain Analysis for Engineering Design, 46(4), 245-266. (2011).

[2] Uenishi, K., & Goji, T. Dynamic fracture and wave propagation in a granular medium: A photoelastic study. Procedia Structural Integrity, 13, 769-774. (2018).

[3] Briñez de León, J. C., Toro, H. A. F., Martínez, A. R., & Bedoya, J. W. B. Análisis de resolución en imágenes de fotoelasticidad: caso carga dinámica. Visión electrónica, 11(1). (2017).

[4] Ajovalasit, A., Petrucci, G., & Scafidi, M. Review of RGB photoelasticity. Optics and Lasers in Engineering, 68, 58-73. (2015).

[5] Quiroga, J. A., & Gonzalez-Cano, A. Separation of isoclinics and isochromatics from photoelastic data with a regularized phase-tracking technique. Applied optics, 39(17), 2931-2940. (2000).

[6] Yoneyama, S., & Arikawa, S. Instantaneous phase-stepping interferometry based on a pixelated micro-polarizer array. Theoretical and Applied Mechanics Letters, 6(4), 162-166. (2016).

[7] Ramakrishnan, V., & Ramesh, K. A novel method for the evaluation of stress-optic coefficient of commercial float glass. Measurement, 87, 13-20. (2016).

[8] Ramakrishnan, V., & Ramesh, K. Scanning schemes in white light Photoelasticity–Part I: Critical assessment of existing schemes. Optics and Lasers in Engineering, 92, 129-140. (2017).

[9] Ramakrishnan, V., & Ramesh, K. Scanning schemes in white light photoelasticity–part II: novel fringe resolution guided scanning scheme. Optics and Lasers in Engineering, 92, 141-149. (2017).

[10] Grewal, G. S., & Dubey, V. N. Inverse problem of photoelastic fringe mapping using neural networks. Measurement Science and Technology, 18(5), 1361. (2007).

[11] Briñez de León, J. C., Martínez, A. R., & Bedoya, J. W. B. High stress concentration analysis using RGB intensity changes in dynamic photoelasticity videos. In 2016 XXI Symposium on Signal Processing, Images and Artificial Vision (STSIVA) (pp. 1-7). IEEE. (2016).

[12] Briñez de León, J. C., Restrepo, A., & Branch, J. W. (2016, September). Time-space analysis in photoelasticity images using recurrent neural networks to detect zones with stress concentration. In Applications of Digital Image Processing XXXIX(Vol. 9971, p. 99712P). International Society for Optics and Photonics. (2016).

[13] Feradov, F. N., & Ganchev, T. D. Spatio-temporal EEG signal descriptors for recognition of negative emotional states. In 2016 XXV International Scientific Conference Electronics (ET) (pp. 1-4). IEEE. (2016).

[14] McCool, P., Chatlani, N., Petropoulakis, L., Soraghan, J. J., Menon, R., & Lakany, H. 1-D local binary patterns for onset detection of myoelectric signals. In 2012 Proceedings of the 20th European Signal Processing Conference (EUSIPCO) (pp. 499-503). IEEE. (2012).

[15] Kumar, T. S., Kanhangad, V., & Pachori, R. B. Classification of seizure and seizure-free EEG signals using local binary patterns. Biomedical Signal Processing and Control, 15, 33-40. (2015).

[16] Kaya, Y., Uyar, M., Tekin, R., & Yıldırım, S. 1D-local binary pattern based feature extraction for classification of epileptic EEG signals. Applied Mathematics and Computation, 243, 209-219. (2014).

[17] Ojala, T., Pietikäinen, M., & Mäenpää, T. Gray scale and rotation invariant texture classification with local binary patterns. In European Conference on Computer Vision (pp. 404-420). Springer, Berlin, Heidelberg. (2000).

[18] Doyle, J. F. Modern experimental stress analysis: completing the solution of partially specified problems. John Wiley & Sons. (2004).

[19] Shang, Wei, Xinhua Ji, and Xiaojing Yang. "Study on several problems of automatic full-field isoclinic parameter measurement by digital phase shifting photoelasticity." Optik-International Journal for Light and Electron Optics126.19 (pp. 1981-1985). (2015):

[20] Magalhães, Pedro Américo Almeida, Cristina Almeida Magalhães, and Ana Laura Mendonça Almeida Magalhães. "Computational methods of phase shifting to stress measurement with photoelasticity using plane polariscope." Optik-International Journal for Light and Electron Optics 130 (pp. 213-226). (2017).

[21] Briñez-de León, J. C., Restrepo-Martínez, A., & Branch-Bedoya, J. W. Computational analysis of Bayer colour filter arrays and demosaicking algorithms in digital photoelasticity. Optics and Lasers in Engineering, 122, 195-208. (2019).